Acoust. Sci. & Tech. **35**, 1 (2014)

PAPER

Development of edge-effect suppression barriers

Yasuhito Kawai* and Masahiro Toyoda†

Department of Architecture, Faculty of Environmental and Urban Engineering, Kansai University, 3–3–35, Yamate-cho, Suita, 564–8680 Japan

(*Received 19 February 2013, Accepted for publication 9 May 2013*)

Abstract: Noise barriers are often very tall alongside highways with heavy traffic. Although these high barriers ensure the desired amount of noise attenuation, they are expensive to install and have a negative effect on the landscape. Consequently, many types of edge-modified noise barriers have been proposed to reduce the necessary height. Herein an alternative noise barrier based on the "edge-effect" suppression technique is proposed, and the sound insulation performance is investigated both theoretically and experimentally. Numerical examples indicate that the diffracted sound is greatly attenuated by suppressing the particle velocity in the region with a large velocity amplitude using a thin absorbing material such as cloth with a gradational distribution in impedance. The experimental and theoretical results of insertion loss are in good agreement, validating the theoretical consideration and effectiveness of the cloth installed at the top of the barrier.

Keywords: Noise barrier, Edge effect, Image method, BEM, Cloth

PACS number: 43.20.El, 43.50.Gf, 43.50.Lj, 43.50.Vt [doi:10.1250/ast.35.28]

1. INTRODUCTION

To shield neighborhoods from road traffic noise and railway noise, the charts proposed by Maekawa [1] and by Koyasu and Yamashita [2] are widely used to obtain the expected insertion loss due to a noise barrier. Although noise barriers are commonly used as a noise prevention measure due to their relatively low cost, good performance, and ease of installation, sometimes very high barriers must be built to achieve the environmental standards. High barriers are disadvantageous because they reduce the attractiveness of the surrounding landscape, inhibit sunshine, and cost more due to the reinforcement necessary for wind resistance. To resolve these issues, many types of edge-modified noise barriers have been proposed [3,4], including sound absorption-type barriers, which trap sound propagating along the absorber surface, phase interference-type barriers, which cancel sound pressure at certain frequency bands, and hybrids of these two types.

The theoretical basis for edge-modified noise barriers is the representation of a diffracted sound field by the line-integral along the barrier edge obtained from Kirchhoff's diffraction theory, which assumes Kirchhoff's boundary conditions [5] via the Maggi-Rubinowicz transformation [6]. Therefore, barriers are designed with the goal of reducing the sound pressure at the barrier edge, which is the integrand of the line integral, by means of sound absorption or phase interference equipment attached at the top of the noise barrier. In this paper, the authors demonstrate via theoretical analysis using boundary integral equations that a region of extremely large particle velocity amplitude, which is omitted in Kirchhoff's diffraction theory, appears in the vicinity of the barrier edge [7] (see Appendix) and that suppressing the large particle velocity in this region decreases the sound level in the diffracted field.

2. THEORETICAL CONSIDERATIONS

2.1. Semi-infinite Barriers

Consider a sound field by a semi-infinite thin rigid barrier where S is the barrier and F is the virtual surface, which is an upward extension of S, as shown in Fig. 1. Then the space is divided into two semi-infinite regions Ω_1 and Ω_2, and one of which (Ω_1) contains point sound source P_s. Let Φ_1 and Φ_2 be the velocity potentials of the sound wave in the two regions Ω_1 and Ω_2 due to the point source. To express the velocity potential Φ_1 at P, the following fundamental solution of Helmholtz's three-dimensional operator considering the mirror image is introduced,

$$G(P,Q) = \frac{\exp(ikr)}{4\pi r} + \frac{\exp(ikr_i)}{4\pi r_i}, \tag{1}$$

where P is a point located inside Ω_1 or on its boundary, Q is a point located on the boundary, $r = |\boldsymbol{r}| = |\overrightarrow{PQ}|$,

*e-mail: kawai@kansai-u.ac.jp
†e-mail: toyoda@kansai-u.ac.jp

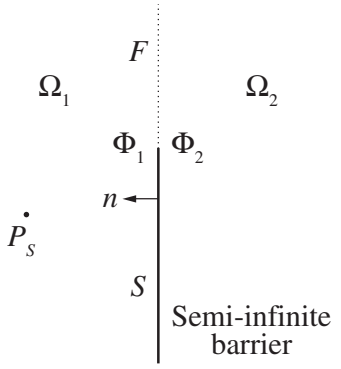

Fig. 1 Sound diffraction by a semi-infinite thin rigid barrier.

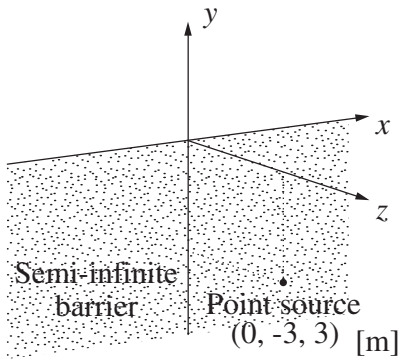

Fig. 3 Calculation of the particle velocity amplitude above a semi-infinite thin rigid barrier.

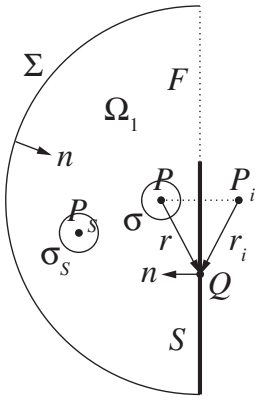

Fig. 2 Derivation of the boundary integral equation for the semi-infinite region Ω_1: Ω_1, which is bounded by infinite sphere Σ of center P and plane boundary $S+F$. n denotes the inward normal. A point source is located at P_s, and a receiving point is at P. P_i denotes the image point of P with respect to the plane $S+F$. Q is a point on $S+F$, while σ_s and σ denote small spheres with centers P_s and P, respectively.

$r_i = |\boldsymbol{r}_i| = |\overrightarrow{P_iQ}|$, and P_i the image point of P with respect to the plane $S+F$ (see Fig. 2). The image method is introduced here so that Φ_1 is expressed using only $\frac{\partial \Phi_1}{\partial n}$ distributed on boundary F. The time factor $\exp(-i\omega t)$ is suppressed throughout, where i is an imaginary unit, ω is the angular frequency, and t is time.

Green's identity or integration by parts can be applied to the region $\Omega_1 - \sigma - \sigma_s$. The region $\Omega_1 - \sigma - \sigma_s$ is bounded externally by S, F, and Σ of center P, which has an infinite radius, and internally by small spheres σ and σ_s, which have respective centers P and P_s and small radii ε. Then taking the limit $\varepsilon \to 0$ leads to

$$\Phi_1(P) = \Phi_D(P) + \Phi_D(P_i) - \iint_F \frac{\partial \Phi_1(Q)}{\partial n} G(P,Q)dS$$
$$= \Phi_D(P) + \Phi_D(P_i) - \frac{1}{2\pi}\iint_F \frac{\partial \Phi_1(Q)}{\partial n}\frac{\exp(ikr)}{r}dS$$
$$(P \in \Omega_1, S, F), \quad (2)$$

where $\frac{\partial}{\partial n}$ denotes the differentiation along the inward normal n to the boundary and Φ_D is the direct wave. Equation (2) holds even when point P lies on the boundary $S+F$ [8]. The integral over Σ is omitted based on the assumption of Sommerfeld's radiation condition [9].

The equation in the other semi-infinite region Ω_2 is derived in a similar manner. Considering a sound source does not exist and the outward normal gives

$$\Phi_2(P) = \iint_F \frac{\partial \Phi_2(Q)}{\partial n} G(P,Q)dS$$
$$= \frac{1}{2\pi}\iint_F \frac{\partial \Phi_2(Q)}{\partial n}\frac{\exp(ikr)}{r}dS$$
$$(P \in \Omega_2, S, F). \quad (3)$$

In Eqs. (2) and (3), when point P lies on boundary F, then P_i overlaps P and the following relations $\Phi_1 = \Phi_2 \stackrel{\text{def}}{=} \Phi$ and $\frac{\partial \Phi_1}{\partial n} = \frac{\partial \Phi_2}{\partial n} \stackrel{\text{def}}{=} \frac{\partial \Phi}{\partial n}$ hold on F. Consequently, subtracting Eq. (3) from Eq. (2) yields

$$\frac{1}{\pi}\iint_F \frac{\partial \Phi(Q)}{\partial n}\frac{\exp(ikr)}{r}dS = 2\Phi_D(P) \quad (P \in F). \quad (4)$$

Equation (4) is the boundary integral equation of the first kind with unknown function $\frac{\partial \Phi}{\partial n}$ on F. Solving integral Eq. (4) and substituting the solution into Eq. (3) gives the diffracted sound field behind the barrier. Note that from Eq. (3), the diffracted sound field is expressed only by the normal derivative of the velocity potential $\frac{\partial \Phi}{\partial n}$ distribution on F, which denotes the component of particle velocity perpendicular to the plane with the opposite sign. Therefore, the design concept for conventional edge-modified barriers, which focuses on controlling the sound pressure instead of the particle velocity, is unreasonable.

As an example, under the conditions shown in Fig. 3, the distribution of the amplitude of the particle velocity along the y-axis solved by Eq. (4) is compared with Kirchhoff's approximation of the boundary value in Fig. 4. In the numerical calculation, the area $0 \le x \le 10\lambda$, $0 \le$

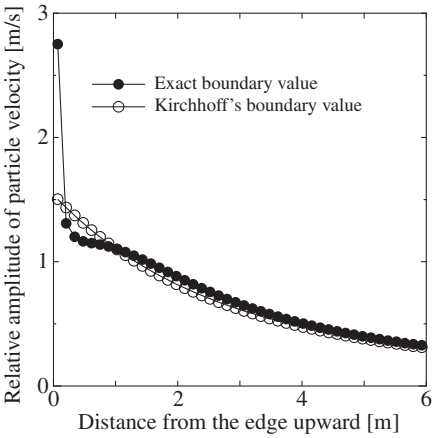

Fig. 4 Particle velocity amplitude along the y-axis at 500 Hz under the conditions shown in Fig. 3.

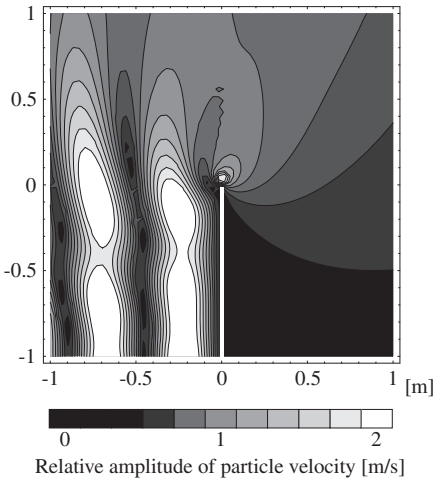

Fig. 5 Distribution of the particle velocity amplitude (normal component) in the yz-plane at 500 Hz under the conditions shown in Fig. 3. Sound source is located in the lower left, and the barrier is located below the center.

$y \leq 10\lambda$ (λ denotes wavelength) is considered because the sound field is symmetrical in the yz-plane and an infinite region cannot be treated numerically. The area was determined based on some preliminary investigations so that the results sufficiently converge and is discretized into constant elements whose dimensions are less than $\lambda/5$ [10]. The manner of determination of integration area and element dimensions is employed throughout in this paper. An omni-directional point source, which gives a unit velocity potential amplitude at a point 1 m from the source, is also used. Figure 4 shows that a region with a very large amplitude of particle velocity exists near the barrier edge. In this paper, the "edge effect" refers to the phenomenon where the incident sound yields a very large amplitude of particle velocity in the vicinity of the edge of a thin object, and is due to the drastic change in sound pressure between the sound-exposed side and the other side at the edge of a thin object. Figure 5 shows the distribution of the particle velocity amplitude of the normal component to the barrier; an isolated area with a large particle velocity appears near the barrier edge. As mentioned previously, because the diffracted field is expressed by the contribution of the particle velocity distribution on F above the barrier, suppressing the prominent particle velocity near the barrier edge by such means as attaching a cloth or thin porous absorber with an appropriate flow resistance should efficiently reduce the diffracted sound.

2.2. Treatment of a Thin Porous Absorbing Material [11]

In the following, the term "cloth" refers to any type of thin porous absorbing material. As shown in Fig. 6, assuming that the flow resistance and relative particle velocity to the cloth are denoted by r_s and v_s, respectively, and that sound pressures in front of and behind the cloth are denoted by p_1 and p_2 gives the following relation

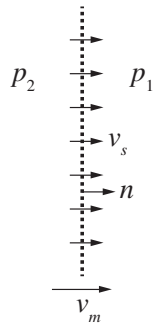

Fig. 6 Impedance of a cloth or a thin absorbing layer.

$$v_s = -\frac{p_1 - p_2}{r_s}. \tag{5}$$

The cloth is also excited by the pressure difference of $p_1 - p_2$. If the surface density of the cloth is denoted by M_s and the vibration velocity by v_m, then the pressure difference can be expressed as

$$-(p_1 - p_2) = M_s \frac{dv_m}{dt} = -i\omega M_s v_m. \tag{6}$$

The particle velocity v at the surface can be expressed by the summation of v_s and v_m as

$$v = v_s + v_m = -\left(\frac{1}{r_s} - \frac{1}{i\omega M_s}\right)(p_1 - p_2). \tag{7}$$

With $Z_r = -(p_1 - p_2)/v$, Eq. (7) yields

$$Z_r = -\frac{p_1 - p_2}{v} = \left(\frac{1}{r_s} - \frac{1}{i\omega M_s}\right)^{-1}. \tag{8}$$

Therefore, the following equation holds

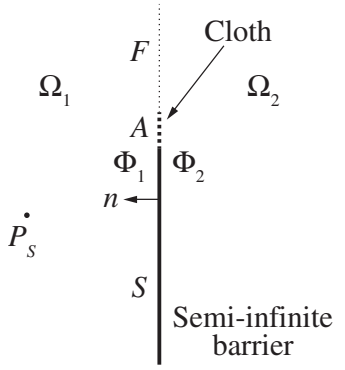

Fig. 7 Edge-effect suppression barrier.

$$v = -\frac{p_1 - p_2}{Z_r} = \frac{i\omega\rho(\Phi_1 - \Phi_2)}{Z_r}. \tag{9}$$

2.3. Semi-infinite Barriers with Zonal Cloths Installed at the Top

Consider a semi-infinite thin rigid barrier along the top where a zonal cloth is set to suppress the large particle velocity amplitude (Fig. 7). In the following, this type of barrier is called as an "edge-effect suppression barrier." Suppose that the surface of the cloth is denoted by A. Because $\Phi_1 = \Phi_2 \overset{\text{def}}{=} \Phi$ on F and $\frac{\partial\Phi_1}{\partial n} = \frac{\partial\Phi_2}{\partial n} \overset{\text{def}}{=} \frac{\partial\Phi}{\partial n}$ on $F + A$, similar to before when P is located on F, the following relation can be obtained

$$\frac{1}{\pi}\iint_{F+A} \frac{\partial\Phi(Q)}{\partial n}\frac{\exp(ikr)}{r}\,dS = 2\Phi_D(P) \quad (P \in F). \tag{10}$$

If P is located on A, then using Eq. (9) gives

$$\begin{aligned}\Phi_1(P) - \Phi_2(P) &+ \frac{1}{\pi}\iint_{F+A} \frac{\partial\Phi(Q)}{\partial n}\frac{\exp(ikr)}{r}\,dS \\ &= -\frac{Z_r}{i\omega\rho}\frac{\partial\Phi(P)}{\partial n} + \frac{1}{\pi}\iint_{F+A} \frac{\partial\Phi(Q)}{\partial n}\frac{\exp(ikr)}{r}\,dS \\ &= 2\Phi_D(P) \quad (P \in A).\end{aligned} \tag{11}$$

Solving Eqs. (10) and (11) simultaneously, $\frac{\partial\Phi}{\partial n}$ on $F + A$ can be calculated. The diffracted sound field can be obtained by the following relation as shown in Eq. (3)

$$\Phi_2(P) = \frac{1}{2\pi}\iint_{F+A} \frac{\partial\Phi(Q)}{\partial n}\frac{\exp(ikr)}{r}\,dS \quad (P \in \Omega_2, S, F, A). \tag{12}$$

3. NUMERICAL EXAMPLES

The result of the 1/10 scale model experiment for an edge-effect suppression barrier and that of theoretical calculation are shown in reference [12]. In the scale model experiment, the barrier is composed of plywood with a thickness of 9 mm and a 50-mm high zonal cloth is attached at the top. In the experiment, the cloth is a curtain fabric with constant flow resistance $r_s = 789\,\mathrm{Ns/m^3}$ and surface density $M_s = 0.66\,\mathrm{kg/m^2}$ throughout the surface. Because the scale model experiment and theoretical calculations are in good agreement, this method appears to be efficient. Many numerical examples demonstrate that the edge-effect suppression barrier has a very good performance for noise shielding efficiency if the cloth has a suitable impedance, which depends on both flow resistance and surface density. However, installation of a cloth with a large and constant impedance to suppress the edge effect near the barrier sufficiently yields another edge effect near the top of the cloth. Figure 8(a) shows an example of the distribution of the particle velocity amplitude of the normal component to such an edge-effect suppression barrier. Two regions with a large particle velocity amplitude near the

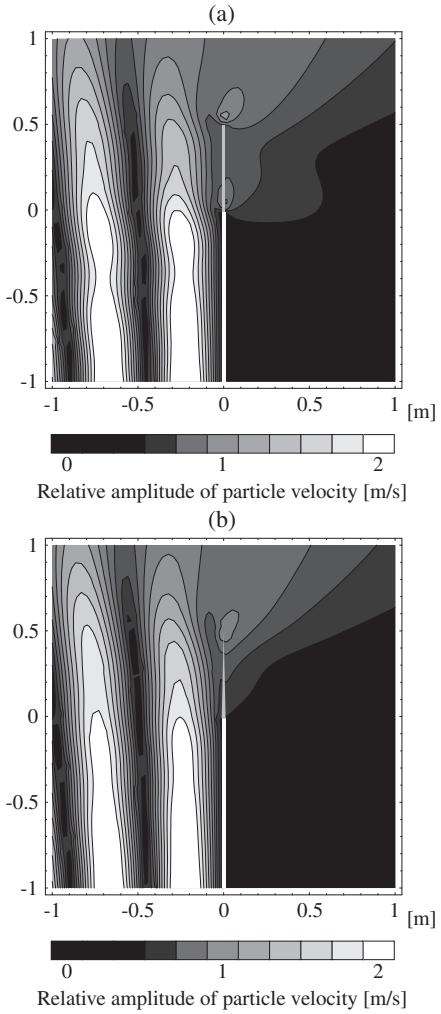

Fig. 8 Distribution of the particle velocity amplitude (normal component) in the yz-plane at 500 Hz under the conditions shown in Fig. 3. (a) Cloth with a constant flow resistance $r_s = 800\,\mathrm{Ns/m^3}$ and surface density $M_s = 1.0\,\mathrm{kg/m^2}$ is attached. (b) Cloth with a gradational distribution in impedance (specimen No. 4 in Table 1) is attached. Sound source is located in the lower left.

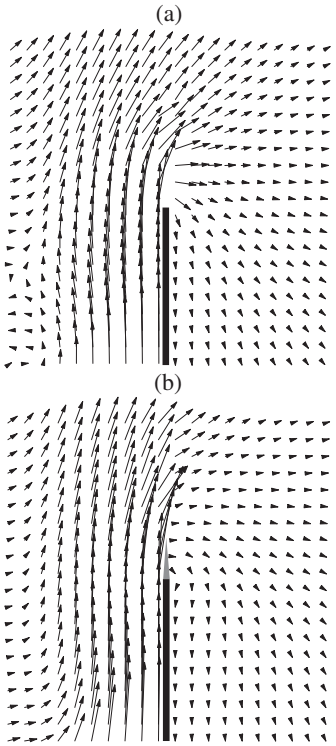

Fig. 9 Time-averaged flow of the sound energy at 125 Hz near the barrier edge for (a) semi-infinite barrier and (b) edge-effect suppression barrier with specimen No. 4 (gradational distribution in impedance).

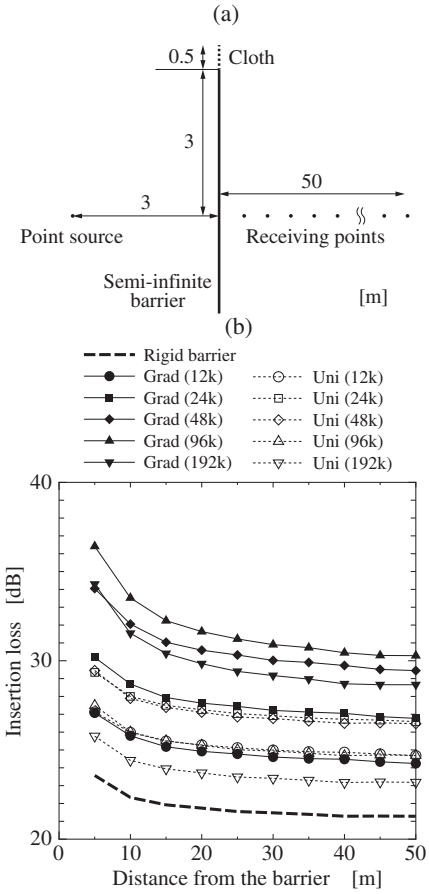

Fig. 10 Calculation of the diffracted sound field due to the edge-effect suppression barrier for (a) positional relationship and dimensions and (b) insertion losses for the A-weighted sound pressure level. Each clipped word in the figure specifies the specimen shown in Table 1. For example, Grad(12k) and Uni(12k) denote specimen number 1 with gradational and uniform characteristics of the physical property, respectively. Dashed line denotes the calculated results for a semi-infinite thin rigid barrier with the same total height as the others.

top and bottom of the cloth can be observed (cf. Fig. 5). As long as a cloth with a constant impedance is used, the sound insulation performance is not improved over a certain limit.

To overcome this limitation, we introduce a cloth whose impedance has a gradational distribution, i.e., the flow resistance and surface density become smaller closer to the top of the cloth and vanish to prevent a drastic change in sound pressure, which causes the edge effect near the top of the cloth. Figure 8(b) shows the distribution of the particle velocity amplitude of the normal component when a cloth with a gradational distribution in impedance is used. The edge effect due to the rigid barrier is sufficiently suppressed, and the additional edge effect near the top of the cloth is also reduced. These results suggest that the diffracted sound field may be further reduced. Figures 9(a) and 9(b) show the time-averaged energy flow diagrams for a semi-infinite rigid barrier and an edge-effect suppression barrier with a cloth possessing a gradational distribution in impedance, respectively. The barrier with a cloth with a gradational distribution transmitted very little energy to the diffracted field.

As numerical examples, the A-weighted sound pressure levels in the diffracted field caused by the road traffic noise spectrum [13] under the conditions shown in Fig. 10(a), where the point source and receiving points are in the same vertical plane ($x = 0$), are calculated from the results for frequencies with 1/18-octave intervals from 100 to 2,500 Hz. The calculations are carried out for several types of specimens installed at the top of the barrier. Table 1 lists the physical properties of the specimens. Figure 10(b)

Table 1 Physical properties of the specimens installed at the top of the barrier. These are the values at the bottom when each specimen has a gradational distribution.

Specimen No.	1	2	3	4	5
Surface density (kg/m^2)	12	24	48	96	192
Flow resistance (Ns/m^3)	400	800	1,600	3,200	6,400

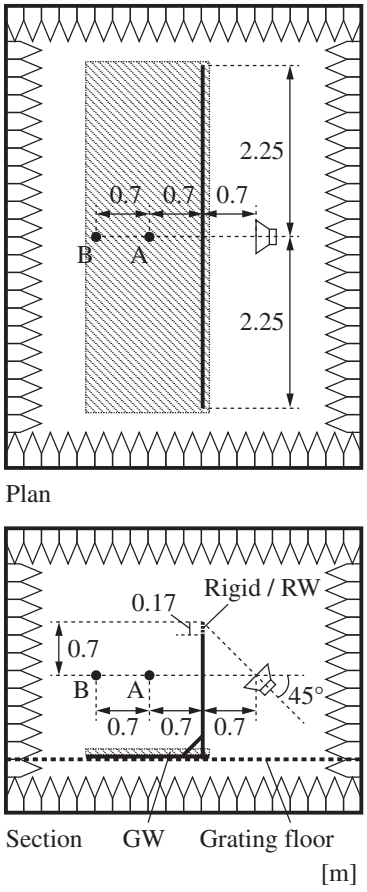

Fig. 11 Experimental configurations.

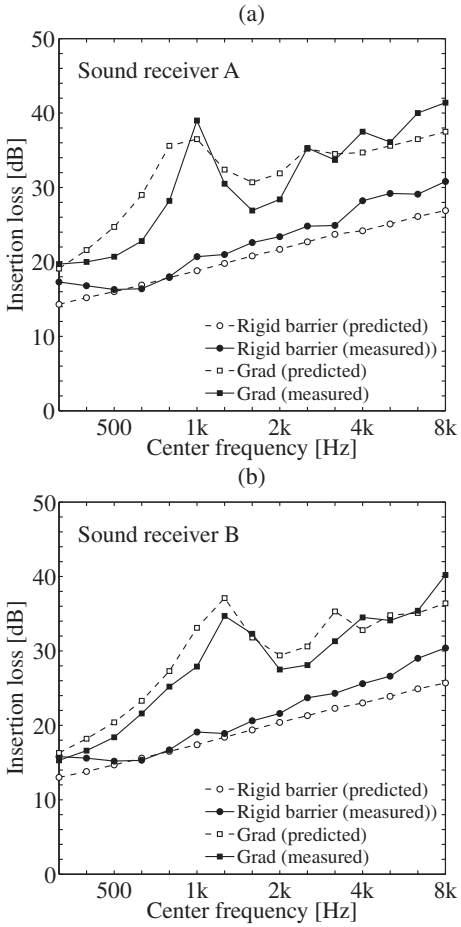

Fig. 12 Comparison between the predicted and measured results of the insertion loss for 1/3-octave bands of (a) sound receiver A and (b) sound receiver B.

shows the insertion losses for the A-weighted sound pressure levels of several edge-effect suppression barriers. Each clipped word in the figure specifies a specimen denoted in Table 1. For example, Grad(12k) and Uni(12k) denote the specimen number 1 with gradational and uniform distributions in impedance, respectively. The dashed line indicates the results for a semi-infinite thin rigid barrier with the same total height. The performance of a cloth with a gradational distribution in impedance is generally better and the attenuation levels increase up to 10 dB. It would be surprising that the sound insulation performance improves only by replacing the upper part of the rigid barrier by such a cloth in which sound is well transmitted.

4. EXPERIMENTAL VALIDATION

To validate the aforementioned theoretical considerations, an experiment in an anechoic chamber was conducted. Figure 11 depicts the experimental configuration. The body of the barrier was composed of 20-mm thick wooden panels. A 20-mm thick rigid wooden panel or a 25-mm thick zonal rock wool at the bottom whose thickness was gradually sharpened along its height was attached at the top of the barrier. Both of them were 170 mm in height. Therefore, the total height of the barrier without a rock wool is the same as that with a rock wool. The flow resistance and the surface density of a 25-mm thick rock wool employed in the experiment were preliminarily measured to be $r_s = 2{,}050\,\mathrm{Ns/m^3}$ and $M_s = 5\,\mathrm{kg/m^2}$, respectively. These parameters were used as the bottom of the cloth in the prediction. The supporting floor was covered by glass wool to avoid sound reflection from the floor. A swept-sine signal was used as the sound source and the impulse responses at the receiving points A and B were obtained. Undesired reflections in the impulse responses were discarded in the time domain allowing for their arrival time and the sound pressures were then processed with a 1/3-octave band filter. Numerical calculations were carried out for frequencies with 1/18-octave intervals, and the energy-averaged value over six values for each 1/3-octave band was obtained. Figure 12 confirms that the experimental and theoretical results of insertion loss are in good agreement, validating the theoretical consideration and effectiveness of the cloth installed at the top of the barrier.

5. CONCLUSION

Herein it is shown that the diffracted sound field due to the placement of a semi-infinite thin rigid barrier is determined by the particle velocity distribution on a virtual plane that is an upward extension of the barrier. The appearance of a region with a large particle velocity amplitude near the top of the barrier is also illustrated. Numerical examples indicate that the diffracted sound is greatly attenuated by suppressing the particle velocity in the region with a large velocity amplitude using a thin absorbing material such as cloth with a gradational distribution in impedance. Thin absorbers with these physical properties can be realized by sharpening the thickness or overlaying multiple pieces of cloth of different heights.

ACKNOWLEDGMENT

We would like to thank the Japan Science and Technology Agency for partly supporting this research. International patent pending (Application No. PCT/JP2012/051471).

REFERENCES

[1] Z. Maekawa, "Noise reduction by screens," *Appl. Acoust.*, **1**, 157–173 (1968).
[2] M. Koyasu and M. Yamashita, "Scale model experiments on noise reduction by acoustic barrier of a straight line source," *Appl. Acoust.*, **6**, 233–242 (1973).
[3] K. Fujiwara and T. Okubo, "Reduction of road traffic noise using edge-modified barriers," *J. INCE/J*, **34**, 347–352 (2010) (in Japanese).
[4] B. Kotzen and C. English, *Environmental Noise Barriers: A Guide to Their Acoustic and Visual Design* (Spon Press, London, 2009), pp. 53–58.
[5] M. Born and E. Wolf, *Principles of Optics*, 5th ed. (Pergamon Press, Oxford, 1975), pp. 378 and 449.
[6] K. Miyamoto and E. Wolf, "Generalization of Maggi-Rubinowicz theory of the boundary diffraction wave I, II," *J. Opt. Soc. Am.*, **52**, 615–637 (1962).
[7] Y. Kawai, "On the approximations of Kirchhoff's boundary conditions," *Proc. 10th ICA* (Sydney), I-4.6 (1980).
[8] Y. Kawai and H. Meotoiwa, "Estimation of the area effect of sound absorbent surfaces by using a boundary integral equation," *Acoust. Sci. & Tech.*, **26**, 123–127 (2005).
[9] B. B. Baker and E. T. Copson, *The Mathematical Theory of Huygens' Principle*, 3rd ed. (AMS Chelsea Publishing, New York, 1987), p. 25.
[10] Architectural Institute of Japan, *Computational Simulation of Sound Environment — Techniques and Applications of Wave-Based Acoustics —* (Maruzen, Tokyo, 2011), pp. 82–84 (in Japanese).
[11] H. Kuttruff, *Room Acoustics*, 4th ed. (Spon Press, London, 2000), pp. 46–51.
[12] Y. Kawai, "Noise shielding efficiency of edge-effect suppression barriers," *Acoust. Sci. & Tech.*, **33**, 204–207 (2012).
[13] "ASJ Prediction Model 2008 for Road Traffic Noise: Report from the Research Committee on Road Traffic Noise in the Acoustical Society of Japan," *J. Acoust. Soc. Jpn.* (*J*), **65**, 179–232 (2009) (in Japanese).

Appendix: KIRCHHOFF'S BOUNDARY CONDITIONS AND RIGOROUS VALUES [7]

In Fig. 1, the approximate boundary values by Kirchhoff [5] for region Ω_2 are expressed as

$$\begin{cases} \Phi_2(P) = \Phi_{\mathrm{D}}(P), & \dfrac{\partial \Phi_2(P)}{\partial n} = \dfrac{\partial \Phi_{\mathrm{D}}(P)}{\partial n} \quad (P \in F) \\ \Phi_2(P) = 0, & \dfrac{\partial \Phi_2(P)}{\partial n} = 0 \quad (P \in S) \end{cases}. \tag{A·1}$$

On the other hand, the rigorous values derived from boundary integral equations are given by

$$\frac{\partial \Phi_2(P)}{\partial n} = \frac{\partial \Phi_{\mathrm{D}}(P)}{\partial n} + \frac{1}{4\pi} \iint_S \tilde{\Phi}(Q) \frac{\exp(ikr)}{r^3} (1 - ikr) dS \quad (P \in F), \tag{A·2}$$

and

$$\Phi_2(P) = \Phi_{\mathrm{D}}(P) - \frac{\tilde{\Phi}(P)}{2} \quad (P \in S), \tag{A·3}$$

where $\tilde{\Phi} = \Phi_1 - \Phi_2$. Thus, the underlined terms are omitted in the approximation of Kirchhoff's boundary conditions. The underlined term in Eq. (A·2) indicates that the particle velocity amplitude becomes large near the barrier edge.